

CHAPTER THREE

FUNDAMENTAL THEORY

Summary

The focus of this chapter is the theory used in this dissertation. This chapter is organized in the following manner:

- Five regions of viscoelastic behavior for solid polymer
- Definition of the terms “transition,” “relaxation,” and “dispersion”
- Dynamic mechanical behavior through the five regions
- Two-phase systems
- Adhesion theories
- Adhesion measurement

3.1 Five Regions of Viscoelastic Behavior

Viscoelastic materials simultaneously exhibit a combination of elastic and viscous behavior. While all substances are viscoelastic to some degree, this behavior is especially prominent in polymers. The five regions of viscoelastic behavior are briefly discussed to provide a broader picture of the temperature dependence of polymer properties [1].

3.1.1 The Glassy Region

The five regions of viscoelastic behavior for linear amorphous polymers are shown in Figure 3.1. In region 1, the polymer is glassy and frequently brittle. Young's modulus for glassy polymers just below the glass transition temperature is surprisingly constant over a wide range of polymers, having the value of approximately 3×10^{10} dynes/cm² (3×10^9 Pa). In the glassy state, molecular motions are largely restricted to vibrations and short-range rotational motions.

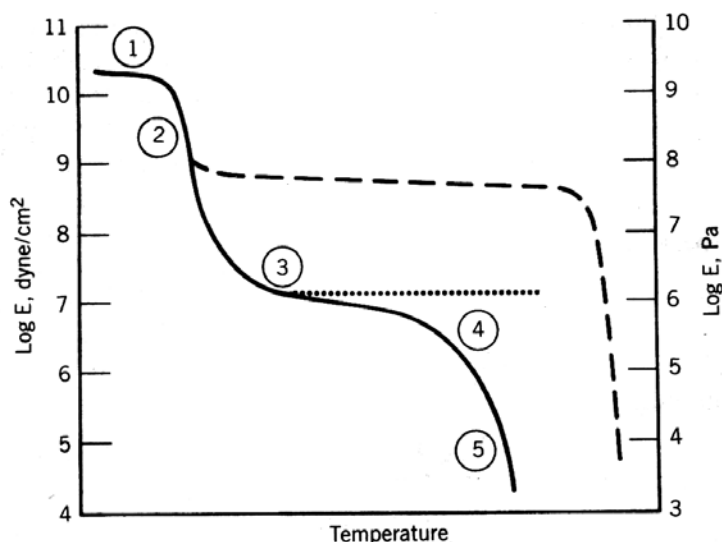


Figure 3.1 Five regions of viscoelastic behavior for a linear, amorphous polymer. Also illustrated are effects of crystallinity (dashed line) and cross-linking (dotted line).

3.1.2 The Glass Transition Region

Region 2 in Figure 3.1 is the glass transition region. Typically, the modulus drops a factor of about 1000 in a 20-30°C range. The behavior of polymers in this region is best described as leathery, although a few degrees of temperature change will obviously affect the stiffness of the leather. For quasistatic measurements such as illustrated in Figure 3.1, the glass transition temperature, T_g , is often taken at the maximum rate of turndown of the modulus at the elbow, where $E \cong 10^{10}$ dyn/cm².

Qualitatively, the glass transition region can be interpreted as the onset of long-range, coordinated molecular motion. While only 1-4 chain atoms are involved in motions below the glass transition temperature, some 10-50 chain atoms attain sufficient thermal energy to move in a coordinated manner in the glass transition region. The number of chain atoms involved in the coordinated motions was deduced by observing the dependence of T_g on the molecular weight between cross-links, M_c , the number of chain atoms was counted.

3.1.3 The Rubbery Plateau Region

Region 3 in Figure 3.1 is the rubbery plateau region. After the sharp drop that the modulus takes in the glass transition region, it becomes almost constant again in the rubbery plateau region, with typical values of 2×10^7 dynes/cm² (2×10^6 Pa). In the rubbery plateau region, polymer exhibit long-range rubber elasticity, which means that the elastomer can be stretched, perhaps several hundred percent, and snap back to substantially its original length on being released.

Two cases in region 3 need to be distinguished:

1. The polymer is linear. In that case, the modulus will drop off slowly, as indicated in Figure 3.1. The width of the plateau is governed primarily by the molecular weight of the polymer; the higher the molecular weight, the longer the plateau (Figure 3.2).
2. The polymer is cross-linked. In this case, the dotted line in Figure 3.1 is followed, and improved rubber elasticity is observed, with the creep portion suppressed. The dotted line follows the equation $E = 3nRT$, where n is the number of active chain segments in the network and RT represents the gas constant times the temperature.

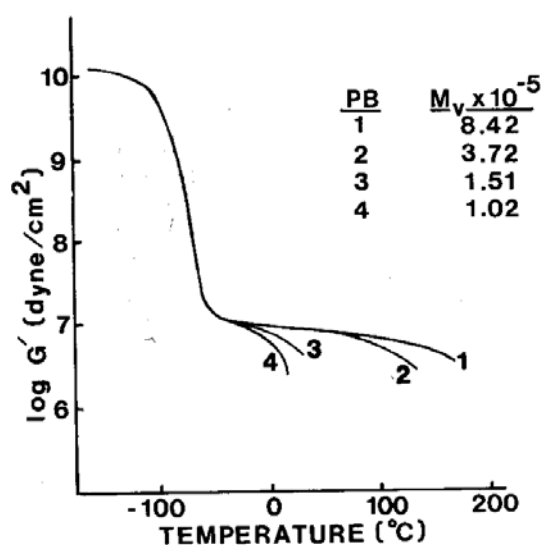


Figure 3.2 Effect of molecular weight on length of plateau.

So far, the discussion has been limited to amorphous polymers. If a polymer is semicrystalline, the dashed line in Figure 3.1 is followed. The height of the plateau is governed by the degree of crystallinity. This is so because of two reasons: first, the crystalline regions tend to behave as a filler phase, and second, because the crystalline regions also behave as a type of physical cross-linking, tying the chains together.

The crystalline plateau extends until the melting point of the polymer. The melting temperature, T_f , is always higher than T_g , T_g being from one-half to two-thirds of T_f on the absolute temperature scale.

3.1.4 The Rubbery Flow Region

As the temperature is raised past the rubbery plateau region for linear amorphous polymers, the rubbery flow region is reached — region 4. In this region, the polymer is marked by both rubber elasticity and flow properties, depending on the time scale of the experiment. For short time scale experiments, the physical entanglements are not able to relax, and the material still behaves rubbery. For longer times, the increased molecular motion imparted by the increased temperature permits assemblies of chains to move in a coordinated manner (depending on the molecular weight), and hence to flow.

It must be emphasized that region 4 does not occur for cross-linked polymers. In that case, region 3 remains in effect up to the decomposition temperature of the polymer (Figure 3.1).

3.1.5 The Liquid Flow Region

At still higher temperatures, the liquid flow region is reached — region 5. The polymer flows readily, often behaving like molasses. The increased energy allotted

to the chains permits them to reptate out through entanglements rapidly and flow as individual molecules.

For semicrystalline polymers, the modulus depends on the degree of crystallinity. The amorphous portions go through the glass transition, but the crystalline portion remains hard. Thus a composite modulus is found. The melting temperature is always above the glass transition temperature. At the melting temperature, the modulus drops rapidly to that of the corresponding amorphous material, now in the liquid flow region. It must be mentioned that modulus and viscosity are related through the molecular relaxation time.

3.2 Definitions of the Terms “Transition,” “Relaxation,” and “Dispersion”

The term “transition” refers to a change of state included by changing the temperature or pressure.

The term “relaxation” refers to the time required to respond to a change in temperature or pressure. It also implies some measure of the molecular motion, especially near a transition condition. Frequently, an external stress is present, permitting the relaxation to be measured.

The term “dispersion” refers to the emission or absorption of energy — that is, a loss peak — at a transition. In practice, the literature sometimes uses these terms somewhat interchangeably.

3.3 Dynamic Mechanical Behavior through the Five Regions

The change in the modulus with temperature has already been introduced in section 3.1. More detail about the transitions is available through dynamic mechanical measurements, sometimes called dynamic mechanical spectroscopy.

While the temperature dependence of G' is similar to that of G , that quantity G'' behaves quite differently. The loss quantities behave somewhat like the absorption spectra in infrared spectroscopy, where the energy of the electromagnetic radiation is just sufficient to cause a portion of a molecule to go to a higher energy state. (Infrared spectrometry is usually carried out by varying the frequency of the radiation at constant temperature.) This exact analogue is frequently carried out for polymers also.

Measurements by dynamic mechanical spectroscopy (DMS) refer to any one of several methods where the sample undergoes repeated small-amplitude strains in a cyclic manner. Molecules perturbed in this way store a portion of the imparted energy elastically and dissipate a portion in the form of heat. The quantity E' , Young's storage modulus, is a measure of the energy stored elastically, whereas E'' , Young's loss modulus, is a measure of the energy lost as heat.

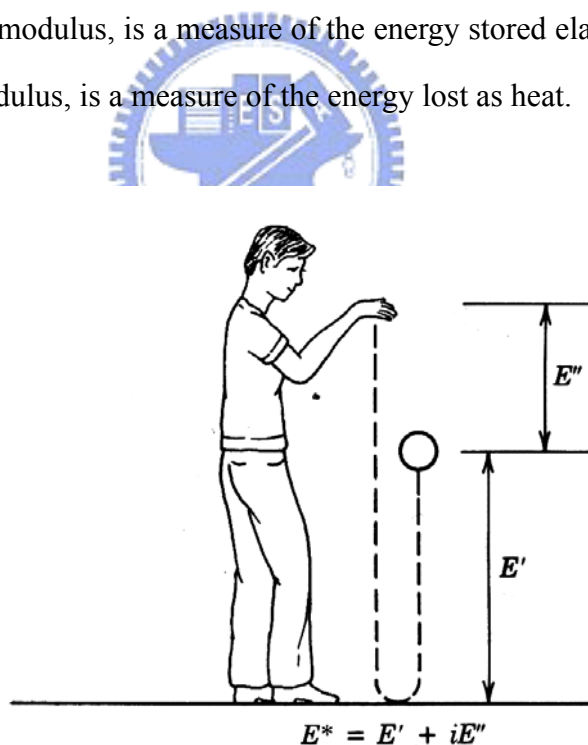


Figure 3.3 Simplified definition of E' and E'' . When a viscoelastic ball is dropped onto a perfectly elastic floor, it bounces back to a height E' , a measure of the energy stored elastically during the collision between the ball and the floor. The quantity E'' represents the energy lost as heat during the collision.

Another equation in wide use is

$$E''/E' = \tan \delta$$

Where $\tan \delta$ is called the loss tangent, δ being the angle between the in-phase and out-of-phase components in the cyclic motion. $\tan \delta$ also goes through a series of maxima. The maxima in E'' and $\tan \delta$ are sometimes used as the definition of T_g .

The dynamic mechanical behavior of an ideal polymer is illustrated in Figure 3.4. The storage modulus generally follows the behavior of Young's modulus as shown in Figure 3.1. In detail, it is subject to equation:

$$E^* = E' + i E''$$

So that the storage modulus is slightly smaller, depending on the value of E'' .

The quantities E'' and $\tan \delta$ display decided maxima at T_g , the $\tan \delta$ maximum appearing several degree centigrade higher than the E'' peak. Also shown in Figure 3.4 is the β peak, generally involving a smaller number of atoms. The area under the peaks, especially when plotted with a linear y axis, is related to the chemical structure of the polymer. The width of the transition and shifts in the peak temperature of E'' or $\tan \delta$ are sensitive guides to the exact state of the material, molecular mixing in blends, and so on.

Also included in the x axis of Figure 3.4 are the long time and the minus log frequency axes. The minus log frequency dependence of the mechanical behavior takes the same form as temperature. As the imposed frequency on the sample is raised, it goes through the glass transition in much the same way as when the temperature is lowered.

For small stresses and strains, if both the elastic deformation at equilibrium and the rate of viscous flow are simple functions of the stress, the polymer is said to exhibit linear viscoelasticity.

The maxima in E'' , G'' , $\tan \delta$ and so on provide a convenient and reproducible measure of each transition's behavior. From an engineering point of view, the intensity of the loss quantities can be utilized in mechanical damping problem such as vibration control.

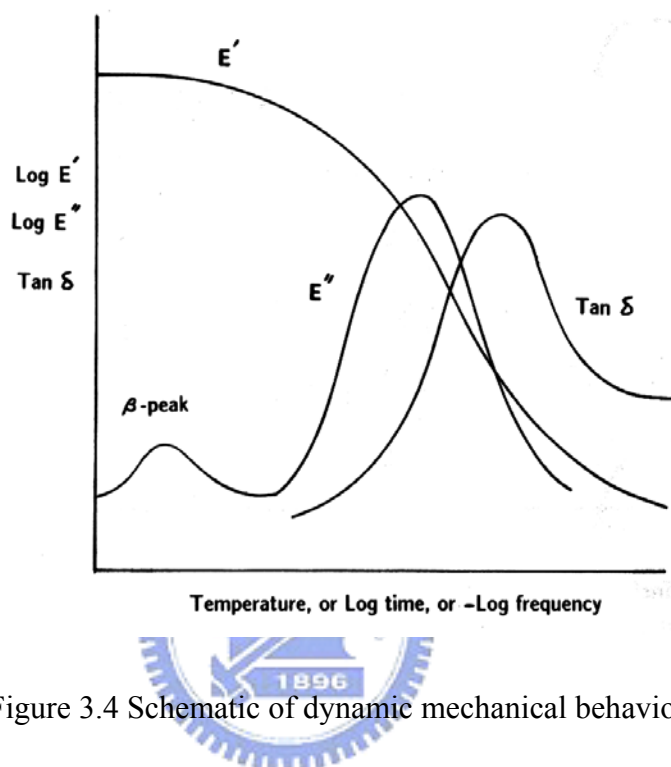


Figure 3.4 Schematic of dynamic mechanical behavior.

3.4 Two-Phase Systems

Most polymer blends, as well as their related graft and block copolymers and interpenetrating polymer networks, are phase-separated. In this case, each phase will exhibit its own T_g . Figure 3.5 illustrates two glass transitions appearing in a series of triblock copolymers of different overall compositions. The intensity of the transition, especially in the loss spectra (E''), is indicative of the mass fraction of that phase.

The storage modulus in the plateau between the two transitions depends both on the overall composition and on which phase is continuous. Electron microscopy shows that the polystyrene phase is continuous in the present case. As the

elastomer component increases (small spheres, then cylinders, then alternating lamellae), the material gradually softens. When the rubbery phase becomes the only continuous- phase, the storage modulus will decrease to about 1×10^8 dynes/cm². If appreciable mixing between the component polymers occurs, the inward shift in the T_g of the two phases can each be observed.

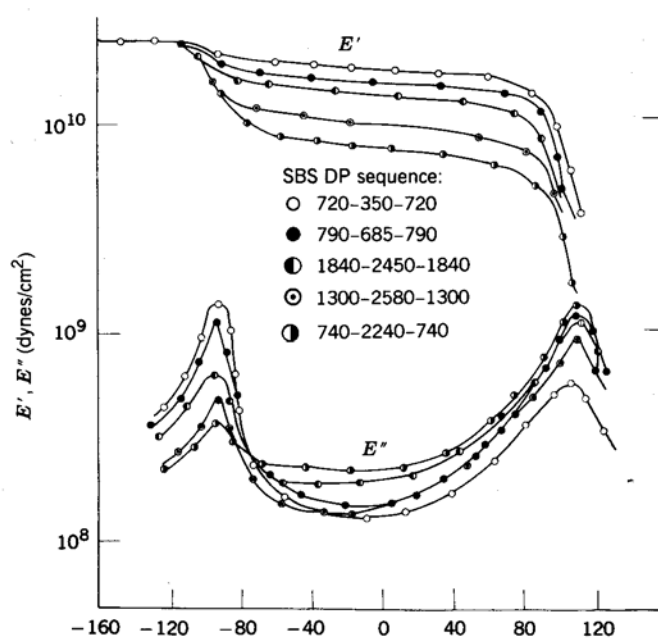


Figure 3.5 Dynamic mechanical behavior of polystyrene-block-polybutadiene-block-polystyrene, a function of the styrene-butadiene mole ratio.

3.5 Adhesion Theories

3.5.1 Mechanical Interlocking

This theory is based on the premise that mechanical interlocking or “hooking” is the cause of adhesion. According to this theory, the adhesion is considered to be due to “tortuous path of fracture” as shown for example, in the scanning electron micrograph of a polyethylene interface surface, which had been formed by depositing the polymer on an anodized aluminum surface. A schematic of the

proposed surface structure of anodized aluminum is also shown in figure 3.6 for comparison [2].

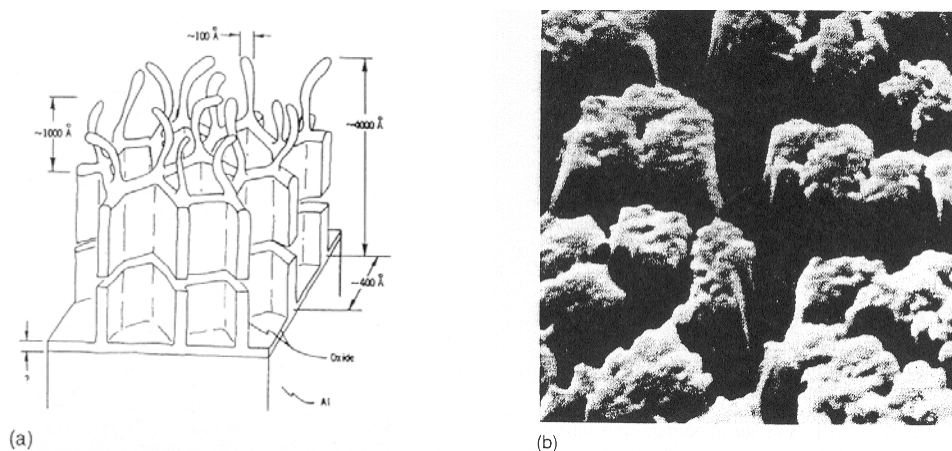


Figure 3.6 (a) Schematic diagram of the proposed structure of anodic oxide film on aluminum. (b) Interface failure surface of polyethylene on anodized aluminum.

3.5.2 Theories Based on Surface Energetic, Wetting and Adsorption

According to this theory, good wetting of the surface is a prerequisite for good overcoat-substrate contact, which can conveniently be characterized by contact angle measurements. It should be emphasized that good wetting (in the extreme case complete spreading) is necessary but not sufficient for good adhesion [2].

3.5.3 Diffusion Theory

This adhesion theory has proven to be invaluable in understanding polymer-polymer adhesion. In this case the materials forming the interface interdiffuse in the interphase region forming an interpenetrated network across the interface [2].

3.5.4 Acid-Base Theory

Acid-base interactions at interface have been studied by various researchers. The

strength of the acid-base interaction at an interface can be estimated using the following expressions:

$$\Delta_A = \text{IEPS} - \text{p}K_{A(A)}$$

$$\Delta_B = \text{p}K_{A(B)} - \text{IEPS}$$

where the subscript A identifies surface reaction with organic acids and the subscript B identifies surface reaction with organic bases. $\text{p}K_{A(A)}$ is the $\text{p}K_A$ of the organic acid and $\text{p}K_{A(B)}$ is that of the organic base. IEPS is the isoelectric point of the surface. Strong acid-base interaction (positive Δ_A or Δ_B) between the overcoat and the substrate is recommended for best adhesion; however, this interaction may also be too strong (large positive Δ) resulting in poor adhesion. For example, although PMDA-ODA PAA on MgO results in strong acid-base interaction at the interface between the acidic PMDA-ODA PAA and the strongly basic MgO, the result is significantly poorer practical adhesion (90 degree peel test) than if the same PAA is coated into Al_2O_3 or SiO_2 (Al_2O_3 is slightly basic, while SiO_2 is acidic). The Δ_A for PAA interaction with inorganic oxide surface (using benzoic acid $\text{p}K_A$ of 4.2 for the PAA) is +7.8 for MgO, +3.8 for Al_2O_3 and -2.2 for SiO_2 . Copper interacts with PAA solution forming a copper carboxylate crosslinking PAA chains and copper is found in the cured PI film ($\Delta_A = +5.3$ for CuO). The acid-base reaction between PAA and MgO is significantly stronger than that between PAA and CuO based on the Δ_A values. MgO is found in PI side of the peel indicating reaction between PAA and MgO causing weakness at the interfacial region. It is therefore suggested that there is optimum acid-base interaction strength at an interface, which would lead to best adhesion [2].

3.5.5 Chemical Bonding

Chemical bonding at an interface is important. A prerequisite for the chemical interaction is closeness of the active sites across the interface. Interaction between active sites will become unimportant when the distance between the reacting

groups is in the excess of 0.5 nm. It is not difficult to build organic contamination layers of this thickness upon exposure to ambient, thus surface cleaning just prior to interface preparation is of primary importance for reliable interfaces.

The covalent bond has high bond energy (70-800 kJ/mol) and is the desired interfacial interaction leading to a reliable bond. Although the ionic bond (electrostatic interaction) also has high bond energy (160-600 kJ/mol), it may suffer from humidity instability renders the interface unreliable in high humidity. Hydrogen bonding and van der Waals forces (neutral molecules, dipole-dipole and multipole interactions) can give strong initial adhesion, but will suffer from exposure to humidity [2].

3.5.6 Weak Boundary Layer Mechanism

Weak boundary layer (WBL) is primarily invoked for explaining poor adhesion and is related to poor cohesive strength of the material in the interfacial region. The WBLs may be caused by several factors:

1. Organic or other contamination on the surface due to ambient exposure (i.e. unclean surface prior to interface preparation).
2. In the case of polymer surfaces a WBL may be formed by the more oriented, perhaps less dense and potentially also lower-molecular-weight material, which may render the surface of the polymer film of lower in-plane fracture toughness than that of the bulk polymer. This may also be the case at the interface, where the polymer coated onto an inorganic substrate may be more ordered and perhaps also of lower in-plane fracture toughness than the bulk polymer would be.

It is evident from the above that no one theory of adhesion would explain all adhesion behaviors observed. There may be a particular theory of adhesion applicable in a given situation [2].

3.6 Adhesion Measurement

Practical adhesion is defined as the force or energy required to disrupt the adhering system irrespective of the locus of failure. This includes the energy required to deform both the film or overcoat and the substrate, as well as the energy dissipated as heat or stored in the film, and the component representative of the actual fundamental adhesion. Practical adhesion can also be described in terms of the time needed to delaminate a coating from a substrate under accelerated testing (such as pressure cooker test) [3-4].

The precise locus of failure (LOF) determination has been a perennial problem in the field of adhesion, since it is dependent on what techniques is used for the analysis. Macroscopically a locus of failure may appear interfacial, while spectroscopic examination would most often suggest cohesive failure in the interphase representing modified layer of one of the materials or a new layer formed by interaction of the two phases (e.g. interdiffused layer or actual chemical reaction). When a clear-cut (macroscopic) cohesive failure is observed, practical adhesion is then a measure of the cohesive strength of the material. In this case the structure can be made more reliable by improving the fracture toughness of the material that failed cohesively (or changing the material to a tougher one).

Fundamental adhesion is the energy required to break the bonds at the weakest plane in the adhering system under the adhesion measurement conditions used. The weakest plane and the energy required may vary as the measurement conditions are changed (e.g. loading conditions of the interface). The fundamental

adhesion does not include the energy used for the deformation of the film or the substrate. If the locus of failure is at the interface, the fundamental adhesion may be called “interfacial fundamental adhesion”. A veritable interfacial failure is a very rare occurrence. Most often the failure occurs in the interphase close to the interface, but not at it.

As a summary of the above.

Practical adhesion = f (fundamental adhesion + other factors)

where “other factors” include film and substrate mechanical properties, stresses, work consumed by plastic deformation and viscous dissipation, rate of interface loading and secondary crack growth.

There are several techniques listed in the literature to assess adhesion. It should be noted that experimentally one can measure only the practical adhesion. The test chosen in this study is 90 degree peel test which is the most popular adhesion test method in microelectronic due to the ease of sample preparation and the ability to measure very high peel forces indicative of good adhesion.

■ 90 Degree Peel Test

The modified peel test is compared to the standard 90 degree peel experiment in Figure 3.7. In both cases (standard and modified 90 degree peel test), the mechanical properties of the peel strip and the substrate, the physical dimensions of the samples, as well as peel rate and ambient will affect the peel strength measured [3].

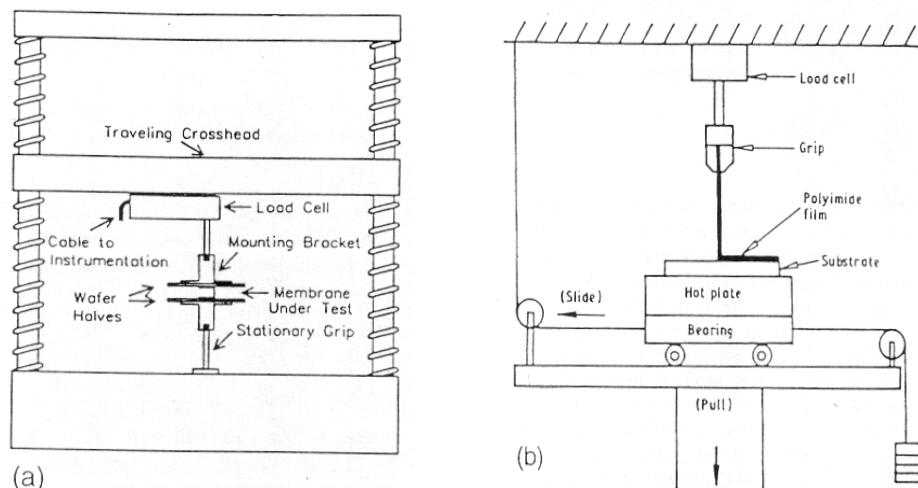


Figure 3.7 (a) Modified 90 degree peel test (b) standard 90 degree peel experiment.

Based on Kim's analysis of the 90 degree peel test adhesion can be determined in some special cases (i.e. where stick-slip behavior is not observed. The stick-slip behavior during peel experiment is explained by Oh et al. in the following way:

Peel-crack propagation is moment controlled process with stress concentration at the peel-crack tip. Thus, during the peel test, the peel strength increases as the radius of curvature of the peel strip at the peel edge decreases (at this point the peel rate is less than the imposed machine rate and the peel is effectively arrested forming a plastic hinge) until the stored strain energy exceeds the fracture resistance at or near the interface at which point the peel-crack propagates. This peel arrestation and propagation from the striations (perpendicular to the peel direction) observed in the polyimide/inorganic system after the peel experiment.

The stick-slip behavior during peeling is observed when adhesion is good and is shown to a function of adhesion, Young's modulus, film thickness and other physical properties of the peel strip and the peeling process [4]. Figure 3.8 shows six PI/ceramic interfaces with different peel adhesion. With high peel strength

(Figure 3.8a-d, f), striations, which are due to stick-slip behavior and are perpendicular to the peel direction, can clearly be seen. The lower the peel strength the smaller the spacing between the striations, resulting finally in continuous peeling without evidence of stick-slip behavior in the case of very poor peel strength, as shown in Figure 3.8 (e).

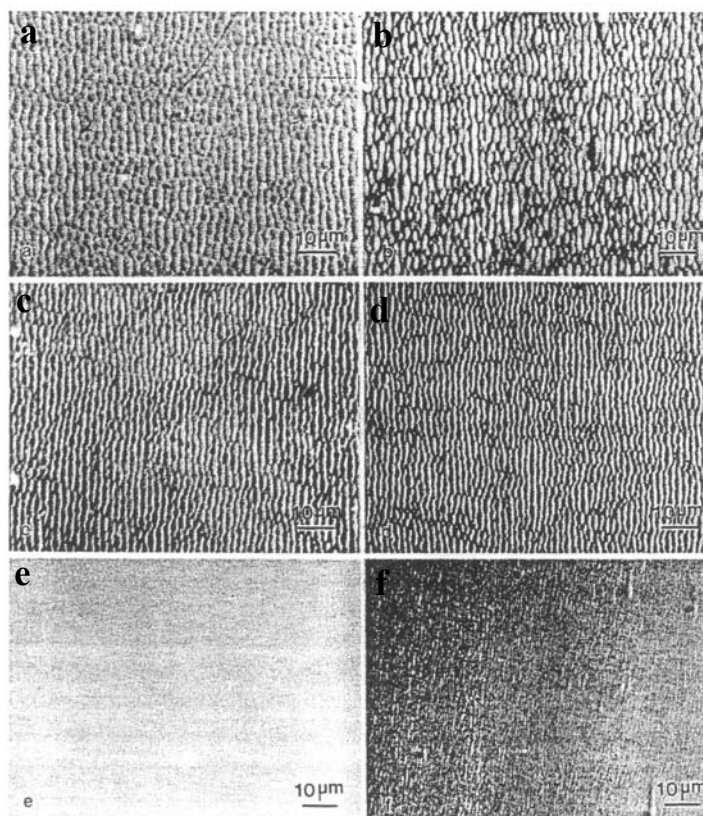


Figure 3.8 Scanning electron micrographs of the peeled surface of (a) PAA PI on SiO_2 580 J/m^2 (b) PAE PI on SiO_2 800 J/m^2 (c) PAA on Al_2O_3 620 J/m^2 (d) PAE PI on Al_2O_3 750 J/m^2 (e) PAA PI on MgO 170 J/m^2 and (f) PAE PI on MgO 530 J/m^2 .

3.7 References

1. L. H. Sperling, *Introduction to Physical Polymer Science*, Chapter 8, John Wiley & Sons, New York (1992).
2. K. L. Mittal ed., *Polyimides: Synthesis, Characterization, and Applications*, Chapter 1-2, Hopewell Junction, New York (1984).
3. M. K. Ghosh, K. L. Mittal ed., *Polyimides: Fundamentals and Applications*, Chapter 20, Marcel Dekker, New York (1996).
4. D. Wilson, H. D. Stenzenberger, P. M. Hergenrother, *Polyimides*, Chapter 6, Blackie, Glasgow and London (1990).

